Si, O-Codoped Carbonized Polymer Dots with High Chemiresistive Gas Sensing Performance at Room Temperature

Yin, Yubo; Gao, Yixun; Wang, Jianqiang; Wang, Quan; Wang, Fengnan; Li, Hao; French, Paddy J.; Paoprasert, Peerasak; Wang, Yao; More Authors

DOI
10.1021/acssensors.4c00617

Publication date
2024

Document Version
Final published version

Published in
ACS Sensors

ACS SENSORS

pubs.acs.org/acssensors

Article

Si, O-Codoped Carbonized Polymer Dots with High Chemiresistive Gas Sensing Performance at Room Temperature

Yubo Yin,[#] Yixun Gao,[#] Jianqiang Wang, Quan Wang, Fengnan Wang, Hao Li, Paddy J French, Peerasak Paoprasert, Ahmad M. Umar Siddiqui, Yao Wang,[*] and Guofu Zhou

Cite This: *ACS Sens.* 2024, 9, 3282−3289

Read Online

ACCESS | Metrics & More | Article Recommendations | Supporting Information

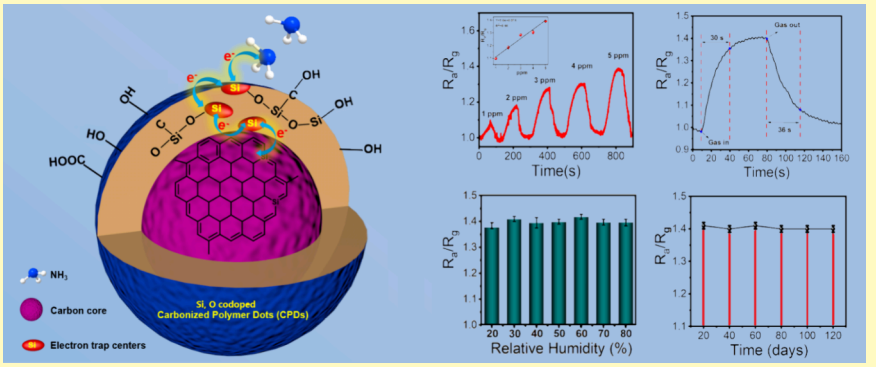

ABSTRACT: A new type of carbonized polymer dot was prepared by the one-step hydrothermal method of triethoxylsilane (TEOS) and citric acid (CA). The sensor made from carbonized polymer dots (CPDs) showed superior gas sensing performance toward ammonia at room temperature. The Si, O-codoped CPDs exhibited superior ammonia sensing performance at room temperature, including a low practical limit of detection (pLOD) of 1 ppm (R_a/R_g: 1.10, 1 ppm), short response/recovery time (30/36 s, 1 ppm), high humidity resistance (less than 5% undulation when changing relative humidity to 80 from 30%), high stability (less than 5% initial response undulation after 120 days), reliable repeatability, and high selectivity against other interferential gases. The gas sensing mechanism was investigated through control experiments and in situ FTIR, indicating that Si, O-codoping essentially improves the electron transfer capability of CPDs and synergistically dominates the superior ammonia sensing properties of the CPDs. This work presents a facile strategy for constructing novel high-performance, single-component carbonized polymer dots for gas sensing.

KEYWORDS: *carbonized polymer dots, gas sensor, ammonia, Si, O-codoping, triethoxylsilane*

With the growing concern for the environment and human health, there is a high demand for hazardous gas monitoring.[1−4] Among these hazardous gases, ammonia (NH_3) gas detection has attracted a great deal of attention in the field of gas sensors.[5] Inhalation of NH_3 above safe levels can cause life-threatening illnesses due to its extreme toxicity and corrosive effects on the mucous membranes and respiratory system. According to the guidelines set by the Occupational Safety and Health Administration (OSHA), the acceptable exposure limits are 25 ppm (ppm) for 8 h and 35 ppm for a duration of 10 min.[6,7] Moreover, NH_3 is also considered as a typical exhaled biomarker for kidney diseases.[8] Therefore, developing high-performance NH_3 sensing materials with low-cost and facile operations is of urgent significance.

In general, optical instruments and absorption spectroscopy are utilized to detect ammonia gas.[9−13] These methods have the advantages of high accuracy, excellent reliability, and low limit of detection (LOD), but the equipment for optical measurement is usually very expensive and large, which restricts their practical application. In recent decades, a large number of literatures have reported various chemiresistive sensors toward ammonia based on metal oxide semiconductors (MOS) and conductive polymer.[14] Most gas sensors based on MOS require relatively high operating temperatures (generally above 150 °C) because oxygen required in the MOS sensing process is only generated at high temperatures.[15] Thus, excessive energy consumption and safety issues could result. As for gas sensors based on conductive polymers, the long response time, weak moisture resistance, and low long-term stability impede their application.[16] Moreover, both metal

Received: March 18, 2024
Revised: May 30, 2024
Accepted: June 3, 2024
Published: June 12, 2024

https://doi.org/10.1021/acssensors.4c00617
ACS Sens. 2024, 9, 3282−3289

Scheme 1. Synthesis Route of the Si, O-CPDs

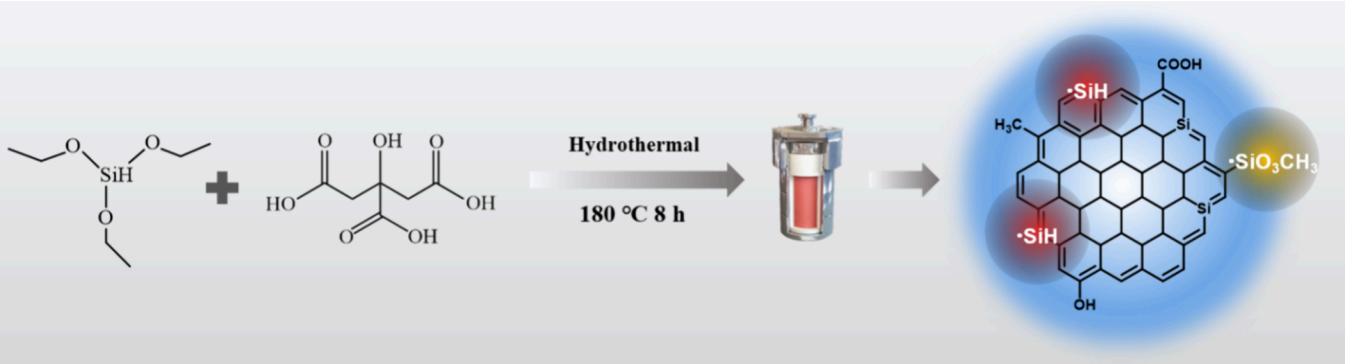

oxides and conductive polymers are not green materials and have a potential hazard to the environment.

Carbonized polymer dots (CPDs) are environmentally friendly and easily prepared zero-dimensional nanomaterials that have shown great potential for gas sensing applications in recent years owing to their excellent optical/electrical properties, high chemical/thermal stability, and tunable surface states.[17−22] Zhang et al. fabricated a nitrogen dioxide (NO_2) chemiresistive sensor through combining CPDs with reduced graphene oxide.[23] Lu et al. decorated In_2O_3 nanoparticles with CPDs and found that the In_2O_3/CPDs composite showed enhanced NO_2 response at the operating temperature of 50 °C.[24] As CPDs increased the density of surface holes and created more nanoheterojunctions to promote the charge transfer in the material, the gas sensitivity of the composite was significantly improved. Apparently, the composites prepared by integrating CPDs and other kinds of materials have shown the promising application prospects of CPDs in the field of gas sensors. However, complex components and multistep reaction would inevitably cause low chemical stability and moisture resistance, which are crucial for gas sensing in various fields. To solve the problem, introducing doping atoms with more stability such as silicon and simplifying the preparation process could be an effective measure.

In this work, we adopted triethoxylsilane and citric acid to synthesize single-component Si, O-codoped CPDs (Si, O-CPDs) through a one-step hydrothermal synthesis. The prepared Si, O-CPDs exhibited superior ammonia sensing properties at room temperature, especially including high humidity resistance and 120 day stability. Four control experiments were conducted to investigate the potential gas sensing mechanism. It is speculated that Si- and O-codoping essentially improves the electron transfer capability of the obtained CPDs and synergistically dominates their superior ammonia sensing properties.

EXPERIMENTAL SECTION

Materials. Triethoxysilane and citric acid were purchased from Innochem (Beijing, China). The stainless steel autoclave was provided by Hua Sin Science Co. (Guangzhou, China). The remaining chemical reagents were of analytical purity and were used directly without additional purification. The Millipore filter (nylon, pore size: 0.22 μm) was sourced from Titan Scientific Co. (Shanghai, China). Additionally, dialysis bags with a molecular weight cutoff (MWCO) of 500 Da (RC type) were obtained from Beijing Yikang Shengshi Biotechnology Co. (Beijing, China).

Synthesis of Si, O-CPDs. For the ammonia sensing performance of Si, O-CPDs, reaction time, reaction temperature, and the molar ratio of the precursor, as the three key factors of preparation, were preferentially optimized. First of all, the reaction time was settled at 6, 8, and 10 h for the same temperature of 180 °C. Besides, a temperature of 200 °C for a time of 8 h was also selected. Figure S1A displays a marked effect of temperature and time on the resulting Si, O-CPDs, which showed the different sensing performance response of Si, O-CPDs prepared at different temperatures and times at the same concentration of ammonia gas. The optimum reaction temperature and time were 180 °C and 8 h, respectively. In addition, the molar ratio of the reaction precursor was investigated because it is a key factor that would affect the gas sensing performance. Figure S1B shows the response performance of the prepared Si, O-CPDs to the same ammonia gas under different molar ratios of reactants. Obviously, with the increase of the mole ratio, the ammonia sensing performance first increased and then decreased. It can be found that when the molar ratio of triethoxylsilane to citric acid is 2:5, the response to ammonia gas is the best. Thus, a heating temperature of 180 °C, a reaction time of 8 h, and a molar ratio of triethoxysilane to citric acid of 2:5 were determined as the optimal preparation conditions for the formation of Si, O-CPDs.

Si, O-CPDs were synthesized via a one-step hydrothermal reaction. During the experimental procedure, 1.0507 g of citric acid (CA) and 350 μL of triethoxysilane (TEOS) were initially dissolved in 10 mL of deionized water to form a homogeneous mixture. This mixture was then poured into a 25 mL poly(tetrafluoroethylene) liner and transferred to a stainless steel autoclave, which was subsequently heated in an oven at 180 °C for 8 h. Upon completion of the reaction, the autoclave was allowed to cool naturally to room temperature. The resultant solution was filtered by using a 0.22 μm microporous membrane and then purified in a dialysis bag for 4 days. Finally, the pure Si, O-CPDs were obtained through lyophilization at a yield of 18.6%.

Characterization. The morphology of Si, O-CPDs was observed by a transmission electron microscope (TEM). The Nanomeasure software was employed to determine the particle sizes of Si, O-CPDs. An X-ray powder diffractometer (XRD) was employed to identify the crystal structure of the samples. Surface group characterization was obtained by Fourier transform infrared spectrophotometer (FTIR). In situ FTIR spectroscopy was performed with a Nicolet iS50. Element composition was confirmed by an X-ray photoelectron spectroscopy (XPS) measurement. Raman spectra were obtained via an inVia Raman microscope. The detailed information on characterizations is provided in the Supporting Information.

Sensor Fabrication. The gas sensing properties were measured by using Ag−Pd interdigital electrodes (IDEs) on ceramic substrates. First, IDEs were cleaned via ultrasonication in alcohol for 30 min before use. A 10 μL aqueous solution of Si, O-CPDs was dropped onto the electrodes and then dried at 60 °C for 15 min.

Gas-Sensing Measurement. A Keithley 2450 electrometer was employed to monitor the resistance changes in the sensors under 1−20 V DC as excitation voltage. Dry ammonia gas (10,000 ppm, Dalian Special Gases Co. Ltd.) taking nitrogen as background was employed as target gas. A complete sensing test involved three sequential steps, as follows: First, the baseline was determined and calibrated in air.

https://doi.org/10.1021/acssensors.4c00617
ACS Sens. 2024, 9, 3282−3289

Second, target gas at a specific concentration was introduced into the chamber and diluted by a built-in fan. Finally, the sensor was recovered by aeration of air after opening the cover of the chamber. The sensor response (S) was calculated by the formula $S = R_a/R_g$, where R_a and R_g, respectively, represent the resistance of the sensors in the atmosphere of air and the target gas. The response/recovery times were defined as the time in which the reading of the gas sensor reaches 90% of the response after exposure to or removal from the gas. The LOD here was defined as the lowest concentration of the target gas distinguishable from the common atmosphere. All the sensing measurements were conducted at 25 °C under a relative humidity (RH) of 25−30% unless otherwise stated.

RESULTS AND DISCUSSION

In this work, as shown in Scheme 1, Si, O-CPDs were produced by the simple hydrothermal method using triethoxysilane and citric acid as the precursors.

As shown in Figure 1A, the obtained granular Si, O-CPDs displayed excellent dispersion with a high density. Figure 1B

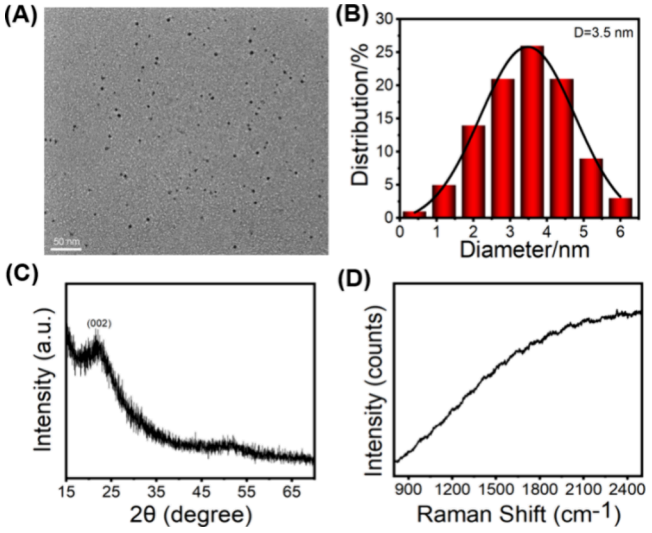

Figure 1. TEM image (A) and size distribution diagram (B) of Si, O-CPDs. XRD pattern (C) and Raman spectrum (D) of Si, O-CPDs.

illustrates that the mean diameter of Si, O-CPD particles was around 3.5 nm with a remarkably narrow distribution, as evidenced by TEM measurement. Distinctly, as shown in Figure 1C, the broad diffraction peak located at 20° illustrated a highly amorphous carbon phase with very few lattices in the obtained Si, O-CPDs.[25] Moreover, Figure 1D shows no distinct D or G band in the Raman spectrum due to the low carbon-lattice-structure content of the Si, O-CPDs,[26] which is the same as the results observed by TEM.

The functional groups present on the surface of the Si, O-CPDs were further characterized by FTIR. As Figure 2A shows, several main absorption peaks can be identified as the O−H stretching vibrations at 3442.7 cm^{-1},[27] the characteristic Si−O stretching vibrations at 794.6 cm^{-1}, the characteristic absorption peak of Si−H at 968.2 cm^{-1},[28] and the C═O stretching vibrations at 1635.5 cm^{-1}.[27] The typical Si−O−Si asymmetric stretching peak was observed at 1105.1 cm^{-1}.[18,29,30] Additionally, XPS measurement was also utilized to analyze the elemental composition and the type of functional groups of the surface of Si, O-CPDs. As illustrated in Figure S2, the atomic composition of the Si, O-CPDs is 10.2% carbon, 58.7% oxygen, and 31.1% silicon. Four peaks

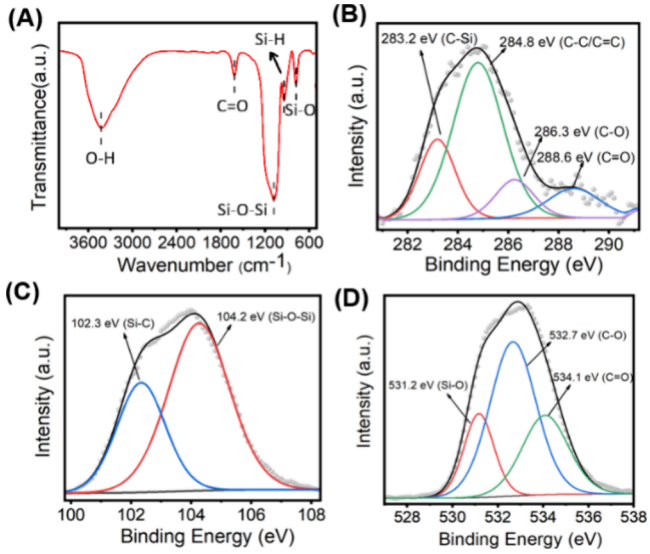

Figure 2. (A) FTIR spectrum of Si, O-CPDs. High-resolution XPS spectra of C 1s (B), Si 2p (C), and O 1s (D) of Si, O-CPDs.

centered at 283.2, 284.8, 286.3, and 288.6 eV were displayed in the high-resolution XPS spectra of C 1s (Figure 2B), which could be assigned to carbon−silicon bonds, carbon−carbon bonds, and carbon−oxygen single and double bonds, respectively.[31−33] The O 1s spectra (Figure 2C) displayed three peaks at 531.2 eV (Si−O), 532.7 eV (C−O), and 534.1 eV (C═O),[34,35] and two peaks at 102.3 eV (Si−C) and 104.2 eV (Si−O−Si) were shown in the Si 2p spectra (Figure 2D).[36,37]

The gas sensing properties were explored by utilizing the prepared samples as sensing materials to prepare sensors on the IDEs. Gas sensing experiments were conducted for ammonia with air as the background gas at an operating temperature of 25 °C.

Figure 3A displays the response−recovery curves of the Si, O-CPDs sensors upon exposure to different concentrations of NH_3 at room temperature, which showed the dynamic response of Si, O-CPDs. There was a discernible response toward a low concentration of NH_3 (1 ppm), which increased with the addition of NH_3. The illustration shows the linear fitting diagram of different NH_3 concentrations, which shows the linear relationship between sensor response and NH_3 concentration. The fitting equation of the sensor based on Si, O-CPDs is $Y = 0.07X + 1.04$ (Y, sensor response; X, gas concentration) in the range of 1−5 ppm. The correlation coefficient (R^2) was 0.97, indicating a positive correlation. The response and recovery times were respectively defined as the time taken to respond to 90% of the full magnitude change in the response/recovery process. For Si, O-CPDs sensors toward 5 ppm ammonia, these two times are 30 and 36 s, respectively.

Reversibility, repeatability, and response rate are critical criteria for gas sensors. Figure 3C shows the response−recovery curve of Si, O-CPDs toward 5 ppm ammonia for five consecutive cycles. The average response value is 1.40, indicating the high reliability and good reversibility of Si, O-CPDs sensing. To date, most room temperature gas sensors still have problems with long response and recovery times. The response and recovery times of Si, O-CPDs toward 5 ppm of NH_3 are relatively shorter (30 and 36 s, respectively). Moreover, the Si, O-CPDs sensor showed excellent selectivity

https://doi.org/10.1021/acssensors.4c00617
ACS Sens. 2024, 9, 3282−3289

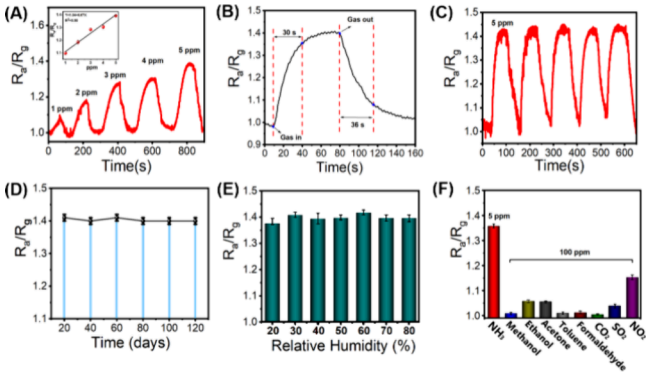

Figure 3. (A) The successive response curve of Si, O-CPDs sensors toward NH_3 in different concentration ranges of 1 to 5 ppm. Inset: corresponding linear fit of the responses of the NH_3 concentration (R^2 = 0.97). (B) Response and recovery time of Si and O-CPDs toward 5 ppm of NH_3. The response time was defined as the time to reach 90% of the maximum response, whereas the recovery time is the time required for the equilibrated resistance to decrease to 10% of the original value after releasing the test gas. (C) The response−recovery curve of Si, O-CPDs sensors toward 5 ppm of NH_3. (D) The 120 day aging test of Si, O-CPDs sensors toward 5 ppm of NH_3. (E) Response of Si, O-CPDs upon exposure to 5 ppm of NH_3 under 20−80% RH. Error bars for the data points lie within the symbols themselves. (F) Sensing selectivity of the Si, O-CPDs sensors toward 5 ppm of NH_3 and 100 ppm of common indoor harmful gases.

among various indoor gases such as NO_2, SO_2, and CO_2 and volatile organic compounds at a concentration of 100 ppm (Figure 3F). Note that Si, O-CPDs based gas sensors show the highest response to 5 ppm ammonia compared to other gases (1.42) (the responses for methanol, ethanol, acetone, and toluene were 1.18, 1.13, 1.08, and 1.07 at 100 ppm, respectively). Meanwhile, the gas-sensitive stability of the prepared Si, O-CPDs material was studied in detail. As demonstrated in Figure 3D, the average response of Si, O-CPDs to 5 ppm ammonia at RT after 120 days of exposure to environmental conditions was 1.40, indicating that Si, O-CPDs have better long-term stability (less than 5% initial response undulation after 120 days). As we know, to realize the practical application of gas sensors, the influence of RH on sensor performance should be considered. The RH range from 20 to 80% was chosen to investigate the impact of different RH on the gas sensing performance of Si, O-CPDs. As shown in Figure 3E, the response of the sensor remains almost the same when the RH increases from 20 to 80%, with only less than 5% undulation. To the best of our knowledge, both the humidity resistance and stability of the Si, O-CPDs based sensing material in this work are the best among the chemiresistive room temperature ammonia sensing materials reported so far. Combined with the reported literature,[48−50] it could be speculated that the high humidity resistance of Si, O-CPDs is attributed to the short amount of time to reach a constant and stable degree of water adsorption on the surface of Si, O-CPDs even at 20% RH.

Table 1 summarizes previous works in terms of metal oxide and non-metal oxide based room temperature NH_3 sensors. The gas sensing performance based on Si, O-CPDs is comparable to those of the listed ammonia gas sensors. In addition, Si, O-CPDs based sensors have relatively shorter response/recovery times and exhibit outstanding humidity resistance and quite high long-term stability. Therefore, the high ammonia sensing performance of Si, O-CPDs makes it a promising material for fabricating room temperature NH_3 sensors.

To further explore the sensing mechanism of the Si, O-CPDs, control experiments were conducted. As listed in Table 2, all the control groups showed no sensing performance toward NH_3 gas compared to Si, O-CPDs, whereas the product in control IV demonstrated a slight response. One possible reason is that oxygen doping would result in a donor level within CPDs so that Si, O-CPDs possessed N-type semiconductor properties.[51] On this basis, according to the semiconductor energy band theory,[52,53] the electron trap centers of silicon atom would easily generate on the surface of CPDs due to the larger atomic radius of silicon atom. As shown in Figure 4, these electron trap centers could constitute electron transmission channels for capturing, storing, and transferring the electrons between the absorbed ammonia on both the surface and inside core of the Si, O-codoped CPDs. Therefore, Si, O-codoping essentially improves the electron transfer capability of CPDs and synergistically dominates the superior ammonia sensing properties of the Si, O-CPDs.

Table 1. Performances of the Comparable Metal Oxide Based and Non-metal Oxide Based Room Temperature NH_3 Gas Sensors[a]

	materials	NH_3 (ppm)	response (R_a/R_g)	response/recovery time (s)	humidity resistance (%)	time stability (days)
metal oxides	ZnO/CuO[14]	1	2.56	2.3/2.1	11−85 (+466%)	150
	MoS_2-Co_3O_4[38]	5	1.65	98/100		
	Pd NPs/TiO_2[39]	5	∼1.13	184/81	40−80 (+10%)	26
	SnO_2-SnS_2[16]	10	1.20	11/>200		
	$Ti_3C_2T_x$/ In_2O_3[40]	5	∼1.12	42/209	15−85 (−40%)	30
	rGO/MoO_3[41]	5	15.11	33/84	0−70 (−20%)	40
	ZnO/graphene[42]	600	11.60	280/300		
	ZnO film[8]	5	3.5	20/25	0−70 (−225%)	12
non-metal oxides	GP-PANI/PVDF[43]	1	1.60	46/198	15−85 (+25%)	17
	PET/PANI[44]	50	1.17	47/-		
	PANi-SnO_2[45]	10	1.07	240/2220		40
	PPy/TfmpoPcCo[46]	5	1.10	22/120	10−95 (−5%)	60
	Ppy/Pd[47]	50	1.13	14/148		
this work	Si, O-CPDs	**5**	**1.40**	30/36	30−80 (<5%)	**120**

[a]Stability refers to the long-term stability. ±: the increase or decrease of the gas response in the range of the humidity change.

https://doi.org/10.1021/acssensors.4c00617
ACS Sens. 2024, 9, 3282−3289

Table 2. Property Comparison of Si, O-CPDs over Four Control CPDs Systems Prepared Using Triethylorthoformate, Triethylsilane, Tetramethylsilane, and Trimethylethoxylsilane instead of Triethoxysilane

Substance	Triethoxysilane (Si,O-CPDs)	Triethylorthoformate (Control I)	Triethylsilane (Control II)	Tetramethylsilane (Control III)	Trimethylethoxylsilane (Control IV)
Structural formula	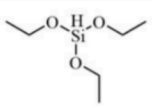	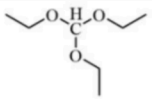	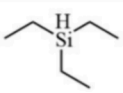		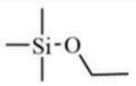
Response (R_a/R_g)	1.40 (5 ppm)	no response (5 ppm)	no response (5 ppm)	no response (5 ppm)	no response (5 ppm)
	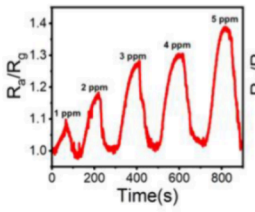	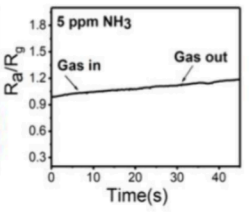	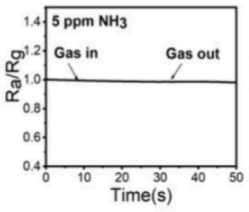	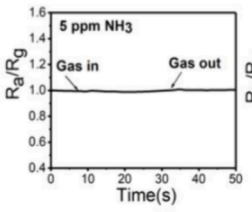	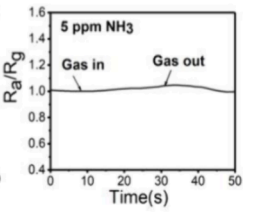

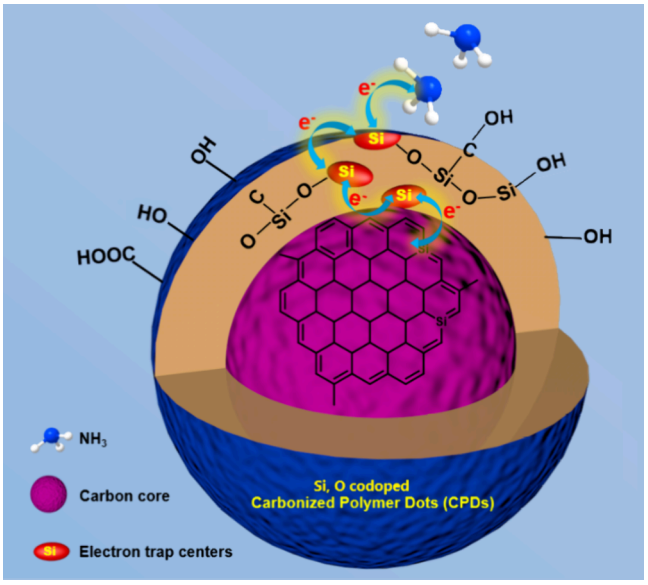

Figure 4. Schematic diagram of the sensing mechanism of the Si, O-codoped CPDs toward NH_3.

In addition, an in situ FTIR measurement was carried out to verify the sensing mechanism from a chemical perspective. The FTIR spectra were collected under a nitrogen atmosphere, as shown in Figure S3A (black line). After the introduction of NH_3 gas into the cell, the intensity of the peak at 1105 cm^{-1} decreased. These results indicated that the Si−O−Si bonds were broken by NH_3 during the sensing process, which is a commonly used chemical reaction in the fields of silane coupling.[54,55] Thus, the change of the chemical structure of Si, O-CPDs would further influence their electrical properties such as resistance. Subsequently, nitrogen purging was carried out to remove NH_3 gas, which led to a degree of reversion of their FTIR spectra (Figure S3B), mainly because the conversion from Si−O−Si to Si−O−H is reversible.

Combining the above two experiments, it could be concluded that Si, O-codoping plays a key role in the sensing process.

CONCLUSIONS

In summary, the Si, O-CPDs were synthesized by a one-step hydrothermal method. The Si, O-CPDs sensors showed superior sensing performance toward NH_3 at room temperature, with high response, relatively short response/recovery time, reliable repeatability, remarkable selectivity, and sensing linearity. More significantly, the sensor showed a high humidity resistance and long-term stability. Moreover, the mechanism study illustrates that it is Si, O-codoping that essentially improves the electron transfer capability of CPDs and synergistically dominates the superior ammonia sensing properties of the CPDs. This work provides a facile strategy for establish high-performance NH_3 sensing systems. It is expected to develop an avenue for the application of single-component carbonized polymer dots in the gas sensing direction.

ASSOCIATED CONTENT

Supporting Information

The Supporting Information is available free of charge at https://pubs.acs.org/doi/10.1021/acssensors.4c00617.

Characterization methods; study of the best preparation conditions of Si, O-CPDs; XPS survey spectrum; and in situ FTIR spectrum (PDF)

AUTHOR INFORMATION

Corresponding Author

Yao Wang − *National Center for International Research on Green Optoelectronics, Guangdong Provincial Key Laboratory of Optical Information Materials and Technology, Institute of Electronic Paper Displays, South China Academy of Advanced Optoelectronics, South China Normal University, Guangzhou 510006, P. R. China;* orcid.org/0000-0002-0713-5018; Email: wangyao@m.scnu.edu.cn

Authors

Yubo Yin − *National Center for International Research on Green Optoelectronics, Guangdong Provincial Key Laboratory of Optical Information Materials and*

https://doi.org/10.1021/acssensors.4c00617
ACS Sens. 2024, 9, 3282−3289

Technology, Institute of Electronic Paper Displays, South China Academy of Advanced Optoelectronics, South China Normal University, Guangzhou 510006, P. R. China

Yixun Gao − *National Center for International Research on Green Optoelectronics, Guangdong Provincial Key Laboratory of Optical Information Materials and Technology, Institute of Electronic Paper Displays, South China Academy of Advanced Optoelectronics, South China Normal University, Guangzhou 510006, P. R. China;* orcid.org/0000-0001-8617-472X

Jianqiang Wang − *National Center for International Research on Green Optoelectronics, Guangdong Provincial Key Laboratory of Optical Information Materials and Technology, Institute of Electronic Paper Displays, South China Academy of Advanced Optoelectronics, South China Normal University, Guangzhou 510006, P. R. China*

Quan Wang − *National Center for International Research on Green Optoelectronics, Guangdong Provincial Key Laboratory of Optical Information Materials and Technology, Institute of Electronic Paper Displays, South China Academy of Advanced Optoelectronics, South China Normal University, Guangzhou 510006, P. R. China*

Fengnan Wang − *Department of Thoracic Oncology, State Key Laboratory of Respiratory Diseases, The First Affiliated Hospital of Guangzhou Medical University, Guangzhou 510006, P. R. China*

Hao Li − *National Center for International Research on Green Optoelectronics, Guangdong Provincial Key Laboratory of Optical Information Materials and Technology, Institute of Electronic Paper Displays, South China Academy of Advanced Optoelectronics, South China Normal University, Guangzhou 510006, P. R. China;* orcid.org/0000-0003-1744-1526

Paddy J French − *BE Laboratory, EWI, Delft University of Technology, Delft 2628CD, The Netherlands*

Peerasak Paoprasert − *Department of Chemistry, Faculty of Science and technology Thammasat University, Pathumthani 12121, Thailand;* orcid.org/0000-0002-6350-9512

Ahmad M. Umar Siddiqui − *Department of Chemistry, Faculty of Science and Arts and Promising Centre for Sensors and Electronic Devices (PCSED), Najran University, Najran 11001, Saudi Arabia*

Guofu Zhou − *National Center for International Research on Green Optoelectronics, Guangdong Provincial Key Laboratory of Optical Information Materials and Technology, Institute of Electronic Paper Displays, South China Academy of Advanced Optoelectronics, South China Normal University, Guangzhou 510006, P. R. China;* orcid.org/0000-0003-1101-1947

Complete contact information is available at: https://pubs.acs.org/10.1021/acssensors.4c00617

Author Contributions

#Y.Y. and Y.G. contributed equally.

Notes

The authors declare no competing financial interest.

■ ACKNOWLEDGMENTS

This work was supported by the National Natural Science Foundation of China (Grant No. 51973070), Science and Technology Program of Guangzhou (No. 2019050001), Guangdong Basic and Applied Basic Research Foundation (2022A1515010577, 2021A1515012420, 2023A1515010814), Innovative Team Project of Education Bureau of Guangdong Province (2018KCXTD009), Guangdong Science and Technology Project-International Cooperation (2022A0505050069), Startup Foundation from SCNU, Guangdong Provincial Key Laboratory of Optical Information Materials and Technology (2023B1212060065), MOE International Laboratory for Optical Information Technologies, and the 111 Project, High-end Foreign Experts Recruitment Program (DL2023030001L).

■ REFERENCES

(1) Lan, R.; Irvine, J. T. S.; Tao, S. Ammonia and related chemicals as potential indirect hydrogen storage materials. *Int. J. Hydrog. Energy* **2012**, *37*, 1482−1494.

(2) Fuerte, A.; Valenzuela, R. X.; Escudero, M. J.; Daza, L. Ammonia as efficient fuel for SOFC. *J. Power Sources* **2009**, *192* (1), 170−174.

(3) Hejze, T.; Besenhard, J. O.; Kordesch, K.; Cifrain, M.; Aronsson, R. R. Current status of combined systems using alkaline fuel cells and ammonia as a hydrogen carrier. *J. Power Sources* **2008**, *176* (2), 490−493.

(4) Comotti, M.; Frigo, S. Hydrogen generation system for ammonia-hydrogen fuelled internal combustion engines. *Int. J. Hydrog. Energy* **2015**, *40*, 10673−10686.

(5) Mani, G. K.; Rayappan, J. B. B. A highly selective and wide range ammonia sensor-Nanostructured ZnO:Co thin film. *Mater. Sci. Eng., B* **2015**, *191*, 41−50.

(6) Mani, G. K.; Rayappan, J. B. B. A highly selective room temperature ammonia sensor using spray deposited zinc oxide thin film. *Sens. Actuators B Chem.* **2013**, *183*, 459−466.

(7) Talwar, V.; Singh, O.; Singh, R. C. ZnO assisted polyaniline nanofibers and its application as ammonia gas sensor. *Sens. Actuators B Chem.* **2014**, *191*, 276−282.

(8) Day, B. A.; Wilmer, C. E. Computational Design of MOF-Based Electronic Noses for Dilute Gas Species Detection: Application to Kidney Disease Detection. *ACS Sensors.* **2021**, *6* (12), 4425−4434.

(9) Peng, W. Y.; Sur, R.; Strand, C. L.; Spearrin, R. M.; Jeffries, J. B.; Hanson, R. K. High-sensitivity in situ QCLAS-based ammonia concentration sensor for high-temperature applications. *Appl. Phys. B: Laser Opt.* **2016**, *122*, 188.

(10) Jin, Z.; Su, Y.; Duan, Y. Development of a polyaniline-based optical ammonia sensor. *Sens. Actuators B Chem.* **2001**, *72*, 75−79.

(11) Mount, G. H.; Rumburg, B.; Havig, J.; Lamb, B.; Westberg, H.; Yonge, D.; Johnson, K.; Kincaid, R. Measurement of atmospheric ammonia at a dairy using differential optical absorption spectroscopy in the mid-ultraviolet. *Atmos. Environ.* **2002**, *36*, 1799−1810.

(12) Kendra, P. E.; Montgomery, W. S.; Mateo, D. M.; Puche, H.; Epsky, N. D.; Heath, R. R. Effect of age on EAG response and attraction of female Anastrepha suspensa (Diptera: Tephritidae) to ammonia and carbon dioxide. *Environ. Entomol.* **2005**, *34*, 584−590.

(13) Yimit, A.; Itoh, K.; Murabayashi, M. Detection of ammonia in the ppt range based on a composite optical waveguide pH sensor. *Sens. Actuators B Chem.* **2003**, *88*, 239−245.

(14) Cheng, C.; Chen, C.; Zhang, H.; Zhang, Y. Preparation and study of ammonia gas sensor based on ZnO/CuO heterojunction with high performance at room temperature. *Mater. Sci. Semicond. Process.* **2022**, *146*, No. 106700.

(15) Lontio Fomekong, R.; Saruhan, B.; Debliquy, M.; Lahem, D. High-temperature NO sensing performance of WO3 deposited by spray coating. *RSC Adv.* **2022**, *12*, 22064−22069.

(16) Xu, K.; Li, N.; Zeng, D.; Tian, S.; Zhang, S.; Hu, D.; Xie, C. Interface Bonds Determined Gas-Sensing of SnO_2-SnS_2 Hybrids to Ammonia at Room Temperature. *ACS Appl. Mater. Interfaces* **2015**, *7*, 11359−11368.

(17) Xia, C.; Zhu, S.; Feng, T.; Yang, M.; Yang, B. Evolution and Synthesis of Carbon Dots: From Carbon Dots to Carbonized Polymer Dots. *Adv. Sci.* **2019**, *6*, No. 1901316.

(18) Pan, K.; Liu, C.; Zhu, Z.; Feng, T.; Tao, S.; Yang, B. Soft-Hard Segment Combined Carbonized Polymer Dots for Flexible Optical Film with Superhigh Surface Hardness. *ACS Appl. Mater. Interfaces* **2022**, *14*, 14504−14512.
(19) Tao, S.; Feng, T.; Zheng, C.; Zhu, S.; Yang, B. Carbonized Polymer Dots: A Brand New Perspective to Recognize Luminescent Carbon-Based Nanomaterials. *J. Phys. Chem. Lett.* **2019**, *10*, 5182.
(20) Huang, J.; Chen, Y.; Rao, P.; Ni, Z.; Chen, X.; Zhu, J.; Li, C.; Xiong, G.; Liang, P.; He, X.; Qu, S.; Lin, J. Enhancing the Electron Transport, Quantum Yield, and Catalytic Performance of Carbonized Polymer Dots via Mn-O Bridges. *Small* **2022**, *18*, No. 2106863.
(21) Yang, X.; Ai, L.; Yu, J.; Waterhouse, G.; Sui, L.; Ding, J.; Zhang, B.; Yong, X.; Lu, S. Photoluminescence mechanisms of red-emissive carbon dots derived from non-conjugated molecules. *Sci. Bull.* **2022**, *67* (14), 1450−1457.
(22) Zhang, Y.; Lu, S. Lasing of carbon dots: Chemical design, mechanisms, and bright future. *Chem.* **2024**, *10* (1), 134−171.
(23) Hu, J.; Zou, C.; Su, Y.; Li, M.; Hu, N.; Ni, H.; Yang, Z.; Zhang, Y. Enhanced NO_2 sensing performance of reduced graphene oxide by in situ anchoring carbon dots. *J. Mater. Chem. C* **2017**, *5*, 6862−6871.
(24) Cheng, M.; Wu, Z.; Liu, G.; Zhao, L.; Gao, Y.; Li, S.; Zhang, B.; Yan, X.; Geyu, L. Carbon dots decorated hierarchical litchi-like In_2O_3 nanospheres for highly sensitive and selective NO_2 detection. *Sens. Actuators B Chem.* **2020**, *304*, No. 127272.
(25) Yang, H.; Liu, Y.; Guo, Z.; Lei, B.; Zhuang, J.; Zhang, X.; Liu, Z.; Hu, C. Hydrophobic carbon dots with blue dispersed emission and red aggregation-induced emission. *Nat. Commun.* **2019**, *10*, 1789.
(26) Wang, Q.; Gao, Y.; Wang, B.; Guo, Y.; Ahmad, U.; Wang, Y.; Wang, Y.; Lu, S.; Li, H.; Zhou, G. S,N-Codoped oil-soluble fluorescent carbon dots for a high color-rendering WLED. *J. Mater. Chem. C* **2020**, *8*, 4343−4349.
(27) Guo, Y.; Jin, X.; Kang, Z.; Wang, L. M. Distinct changes of Debye relaxation in primary and secondary monoalcohols by carbon nano-dots. *J. Mol. Liq.* **2020**, *297*, No. 111738.
(28) Song, Y.; Wang, L.; Wang, X.; Bian, K.; Yang, Q.; Li, Y. Preparation of a New Superhydrophobic Nanofiber Film by Electrospinning Polystyrene Mixed with Ester Modified Silicone Oil. *J. Appl. Polym. Sci.* **2014**, *131*, 40718.
(29) Kim, Y.; Choi, G.-M.; Bae, J.; Kim, Y.; Bae, B. S. High-Performance and Simply-Synthesized Ladder-Like Structured Methacrylate Siloxane Hybrid Material for Flexible Hard Coating. *Polymers* **2018**, *10*, 449.
(30) Wang, J.; Gao, Y.; Chen, F.; Zhang, L.; Li, H.; de Rooij, N. F.; Umar, A.; Lee, Y.-K.; French, P. J.; Yang, B.; Wang, Y.; Zhou, G. Assembly of Core/Shell Nanospheres of Amorphous Hemin/Acetone-Derived Carbonized Polymer with Graphene Nanosheets for Room-Temperature NO Sensing. *ACS Appl. Mater. Interfaces* **2022**, *14*, 53193−53201.
(31) Qu, S.; Liu, X.; Guo, X.; Chu, M.; Zhang, L.; Shen, D. Amplified Spontaneous Green Emission and Lasing Emission From Carbon Nanoparticles. *Adv. Funct. Mater.* **2014**, *24*, 2689.
(32) Feng, T.; Zeng, Q.; Lu, S.; Yan, X.; Liu, J.; Tao, S.; Yang, M.; Yang, B. Color-Tunable Carbon Dots Possessing Solid-State Emission for Full Color Light-Emitting Diodes Applications. *ACS Photonics* **2018**, *5*, 502.
(33) Guo, Y.; Wang, Q.; Li, H.; Gao, Y.; Xu, X.; Tang, B.; Wang, Y.; Yang, B.; Lee, Y.-K.; French, P. J.; Zhou, G. Carbon Dots Embedded in Cellulose Film: Programmable, Performance-Tunable, and Large-Scale Subtle Fluorescent Patterning by in Situ Laser Writing. *ACS Nano* **2022**, *16*, 2910.
(34) Sun, S.; Zhang, L.; Jiang, K.; Wu, A.; Lin, H. Toward High-Efficient Red Emissive Carbon Dots: Facile Preparation, Unique Properties, and Applications as Multifunctional Theranostic Agents. *Chem. Mater.* **2016**, *28*, 8659.
(35) Gao, Y.; Wang, J.; Feng, Y.; Cao, N.; Li, H.; de Rooij, N. F.; Umar, A.; French, P. J.; Wang, Y.; Zhou, G. Carbon-Iron Electron Transport Channels in Porphyrin-Graphene Complex for ppb-Level Room Temperature NO Gas Sensing. *Small* **2022**, *18*, No. 2103259.
(36) Zhan, Y.; Shang, B.; Chen, M.; Wu, L. One-Step Synthesis of Silica-Coated Carbon Dots with Controllable Solid-State Fluorescence for White Light-Emitting Diodes. *Small* **2019**, *15*, No. 1901161.
(37) Cao, N.; Wang, Q.; Zhou, X.; Gao, Y.; Feng, Y.; Li, H.; Bai, P.; Wang, Y.; Zhou, G. Where is the best substitution position for amino groups on carbon dots: a computational strategy toward long-wavelength red emission. *J. Mater. Chem. C* **2021**, *9*, 14444−14452.
(38) Zhang, D.; Jiang, C.; Li, P.; Sun, Y. Layer-by-Layer Self-assembly of Co_3O_4 Nanorod-Decorated MoS_2 Nanosheet-Based Nanocomposite toward High-Performance Ammonia Detection. *ACS Appl. Mater. Interfaces* **2017**, *9*, 6462−6471.
(39) Su, P.-G.; Chen, F.-Y.; Wei, C.-H. Simple one-pot polyol synthesis of Pd nanoparticles, TiO_2 microrods and reduced graphene oxide ternary composite for sensing NH_3 gas at room temperature. *Sens. Actuators B Chem.* **2018**, *254*, 1125.
(40) Zhou, M.; Han, Y.; Yao, Y.; Xie, L.; Zhao, X.; Wang, J.; Zhu, Z. Fabrication of $Ti_3C_2T_x/In_2O_3$ nanocomposites for enhanced ammonia sensing at room temperature. *Ceram. Int.* **2022**, *48*, 6600−6607.
(41) Ou, Y.; Zhou, Y.; Guo, Y.; Zhu, X.; Liu, B.; Gao, C. Room-temperature high-performance ammonia gas sensing based on rGO nanosheets/MoO_3 nanoribbons nanocomposites film. *FlatChem.* **2022**, *32*, No. 100333.
(42) Hang, T.; Wu, J.; Xiao, S.; Li, B.; Li, H.; Yang, C.; Yang, C.; Hu, N.; Xu, Y.; Zhang, Y.; Xie, X. Anti-biofouling NH_3 gas sensor based on reentrant thorny ZnO/graphene hybrid nanowalls. *Microsyst. Nanoeng.* **2020**, *6*, 41.
(43) Wu, Q.; Shen, W.; Lv, D.; Chen, W.; Song, W.; Tan, R. An enhanced flexible room temperature ammonia gas sensor based on GP-PANI/PVDF multi-hierarchical nanocomposite film. *Sens. Actuators B Chem.* **2021**, *334*, No. 129630.
(44) Ma, J.; Fan, H.; Li, Z.; Jia, Y.; Yadav, A. K.; Dong, G.; Wang, W.; Dong, W.; Wang, S. Multi-walled carbon nanotubes/polyaniline on the ethylenediamine modified polyethylene terephthalate fibers for a flexible room temperature ammonia gas sensor with high responses. *Sens. Actuators B Chem.* **2021**, *334*, No. 129677.
(45) Khuspe, G. D.; Navale, S. T.; Bandgar, D. K.; Sakhare, R. D.; Chougule, M. A.; Patil, V. B. SnO_2 nanoparticles-modified Polyaniline Films as Highly Selective, Sensitive, Reproducible and Stable Ammonia Sensors. *Electron. Mater. Lett.* **2014**, *10*, 191−197.
(46) Gai, S.; Wang, B.; Wang, X.; Zhang, R.; Miao, S.; Wu, Y. Ultrafast NH_3 gas sensor based on phthalocyanine-optimized non-covalent hybrid of carbon nanotubes with pyrrole. *Sens. Actuators B Chem.* **2022**, *357*, No. 131352.
(47) Hong, L.; Li, Y.; Yang, M. Fabrication and ammonia gas sensing of palladium/polypyrrole nanocomposite. *Sens. Actuators B Chem.* **2010**, *145* (1), 25−31.
(48) Song, L.; Zhang, H.; Chen, J.; Li, Z.; Guan, M.; Qiu, H. Imidazolium ionic liquids-derived carbon dots-modified silica stationary phase for hydrophilic interaction chromatography. *Talanta* **2020**, *209*, No. 120518.
(49) Cai, T.; Zhang, H.; Rahman, A.; Shi, Y.; Qiu, H. Silica grafted with silanized carbon dots as a nano-on-micro packing material with enhanced hydrophilic selectivity. *Microchim Acta* **2017**, *184*, 2629−2636.
(50) Li, Y.; Bellani, C.; Yebo, N.; Dendooven, J.; Seo, J. W.; Detavernier, C.; Baets, R.; Martens, J. A.; Pulinthanathu Sree, S. Nanoporous Silica−Alumina Films Fabricated on Silicon Photonic Chips for Selective Ammonia Sensing. *ACS Appl. Nano Mater.* **2022**, *5*, 16126−16135.
(51) Goudarzi, M.; Parhizgar, S. S.; Beheshtian, J. Electronic and optical properties of vacancy and B, N, O and F doped graphene: DFT study. *Opto-Electron. Rev.* **2019**, *27*, 130−136.
(52) Singh, M.; Goyal, M.; Devlal, K. Size and shape effects on the band gap of semiconductor compound nanomaterials. *J. Taibah Univ. Sci.* **2018**, *12*, 470−475.
(53) Shen, H.; Zhen, B.; Fu, L. Topological Band Theory for Non-Hermitian Hamiltonians. *Phys. Rev. Lett.* **2018**, *120*, No. 146402.

https://doi.org/10.1021/acssensors.4c00617
ACS Sens. 2024, 9, 3282−3289

(54) Harris, M. T.; Brunson, R. R.; Byers, C. H. The base-catalyzed hydrolysis and condensation reactions of dilute and concentrated TEOS solutions. *J. Non-Cryst. Solids* **1990**, *121*, 397−403.
(55) Cihlar, J. Hydrolysis and polycondensation of ethyl silicates. 1. Effect of pH and catalyst on the hydrolysis and polycondensation of tetraethoxysilane (TEOS). *Colloid Surface A* **1993**, *70*, 239−251.

https://doi.org/10.1021/acssensors.4c00617
ACS Sens. 2024, 9, 3282−3289